Analogue Experiments of Subduction VS. Collision Processes: Insight for the Iranian Tectonics

V. Regard[1, 4], O. Bellier[1], J. Martinod[2], and C. Faccenna[3]

1. Centre Européen de Recherche et d'Enseignement en Géosciences de l'Environnement-CEREGE, UMR CNRS 6635, Université Aix-Marseille III, Europôle de l'Arbois BP80, 13545 Aix-en-Provence cedex 4, France
2. Laboratoire des Mécanismes et Transferts en Géologie-LMTG, UMR5563CNRS/ Université Toulouse III/IRD, 14 av. E. Belin, 31400 Toulouse, France
3. Dipartimento di Scienze Geologiche, Università Roma tre, Largo S. L. Murialdo 1, 00146, Roma, Italy
4. Now at Laboratoire des Mécanismes et Transferts en Géologie-LMTG, UMR5563CNRS/Université Toulouse III/IRD, 14 av. E. Belin, 31400 Toulouse, France, email: regard@lmtg.obs-mip.fr

ABSTRACT: *The behavior of subduction-collision transition is investigated, using laboratory experiments. These experiments help understanding the tectonics at the transition between the Zagros collision ranges and the Makran emerged accretionary prism in south-eastern Iran. Lithospheric plates are modeled by sand-silicone plates floating on glucose syrup, and the density contrast between oceanic and continental lithospheric plates and asthenosphere is reproduced. Analogue experiments model the convergence between two lithospheric plates, a small continent indenting a large continental plate. These experiments provide evidence for surface deformation in front of the indenter and above the oceanic subduction zone that depend on the behavior of the slab below the collision zone. Slab break-off following the subduction of the small continent favors the indentation process, because it results in an increasing compression in front of the indenter, and extension above the neighboring oceanic subduction, both of them being responsible for the appearance of the indenter-like geometry of the plate boundary. When the slab does not deform significantly at depth, in contrast, the closure of the oceanic domain in front of the indenter is followed by a longer period of continental subduction, during which the tectonic regime within the large continent remains quite homogeneous. In south-east Iran, the transition between Zagros and Makran is accommodated over a large area, from the Hormoz strait to the East-Iranian ranges; it suggests that the slab is continuous at depth. On the contrary, the Chaman fault zone between Makran and Himalayas is a narrow zone and is clearly related to a tear away of the underlying slab.*

Keywords: Iran; Subduction; Collision; Analogue experiments; Tectonics; Zagros; Makran; Break-off; Lithosphere; Continent

1. Introduction

Indentation is defined as the collision of a relatively small "indenter" with a large continental domain, generally flanked on its sides by subduction zones. The "indenter" is globally buoyant and has drifted towards the indented continent by subduction of the oceanic domain that initially separated them. Presently, many studies argue in favor of combined or successive vertical/horizontal extrusion to explain deformation related to collision [10]. Consequently, to understand collision processes, it appears

necessary to look at the indentation mechanisms in 3 dimensions. The Makran subduction zone is flanked by two indenters, Arabia and India. Indentation is expressed differently to the West (transition toward the Zagros) than to the East (transition toward Himalayas).

The tectonic process driving and accompanying indentation has been investigated especially for those aspects concerning the way the upper plate deforms. It has been pointed out that a major role is played by the strength of the upper plate, providing the possibilities to squeeze and thicken the crust or producing the lateral escape of crustal blocks along strike-slip faults, e.g. [16, 24]. In particular, it seems that a tectonic escape must be allowed by the presence, at the sides of the indented continent of free boundaries, i.e., not exerting any confining force. Indeed, if one compares subduction zones, it is evident that the effects of the subduction dynamics vary, for the upper plate, from compressional to extensional deformation (for example Andes and Aegean domain, e.g. [14, 23]). Consequently, the role played by subduction zones laterally bounding the "indenter" must be of high importance, but has not received the interest it deserves.

We present laboratory experiments performed to define the role of subduction in the tectonics of indentation. These experiments are part of an experimental program devoted to the investigation of the physical parameters that drive subduction/ collision processes. We first describe 2*D* experiments to illustrate the way continental lithosphere subducts prior to collision, and following oceanic subduction. The results of this set of experiments show that the possibility for the continent to subduct is related to the pull exerted by the previously subducted oceanic lithosphere, and therefore to the way the slab deforms at depth. Our results were expressed by means of two dimensionless numbers (*F*) where the slab pull force is normalized to the strength of the slab: Favorable conditions for continental subduction require low values of *F*, or in other words, the oceanic slab is more prone to maintain its integrity and to exert a higher pull on the subducting continent. If this analysis applies well to the central part of the Arabia-Eurasia collision zone, it is worth noting that side effects would change its conclusions for external zones, e.g. Aegean and south-eastern Iran. To complement this analysis, we developed a more complex 3*D* configuration with a lateral transition from oceanic to continental subduction.

2. Experiments on the Transition Subduction-Collision

2.1. Experimental Setup

We simulate the stratified lithospheric rheological profile, e.g. [17], by constructing a brittle-ductile layered model, with a sand mixture to model the brittle behavior of the upper crust and silicone putty to model the ductile behavior of the lower crust and mantle lithosphere. The sand-silicone layering rests on honey, which simulates the upper mantle, see Figure (1). Two different kinds of sand-silicone layers were used, either lighter or denser than the glucose syrup, to represent continental or oceanic lithospheres, respectively. Continental and oceanic plates differ in thickness, density and viscosity of the upper silicone layer, and in thickness and density of the sand layer. The lower boundary of the box approximates a high gradient viscosity transition.
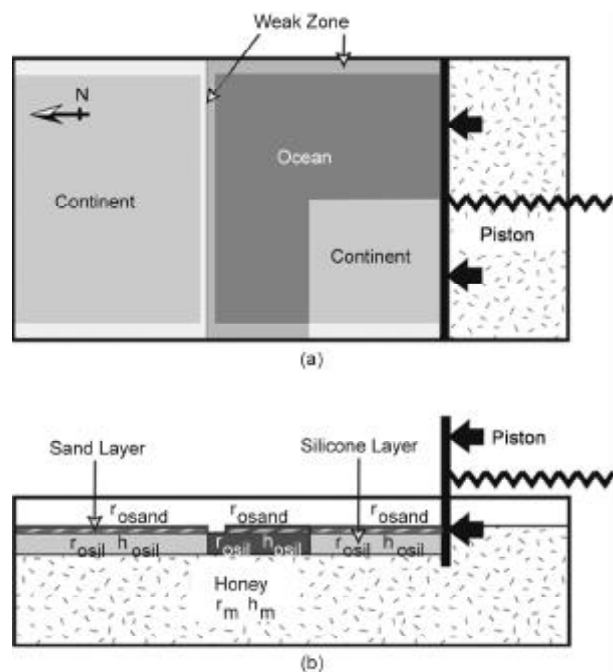

Figure 1. Experimental setup: (a) upper view and (b) cross-section of the western part of the model. Sand/silicone plates modeling the lithosphere are lying above honey that represents the asthenosphere. These plates are lighter or denser than honey, to represent continental or ocean lithosphere, respectively. The setup presented is 3-dimensional in the sense that at south the subducting plate is divided into a continental part (SW) and an oceanic part (SE). Close to the trench however the southern plate is oceanic from east to west to allow a 2D subduction initiation. The piston is pushing northward at a constant velocity of 4.4mm/h scaled to represent 2.3cm/yr in nature. The oceanic plate will subduct below the northern continent, the subduction place being controlled by the removal of a 1 cm-wide band of sand that weakens the northern margin of the oceanic plate.

Models are constructed inside a rectangular Plexiglas tank (50*cm* long, 30*cm* wide and 11 to 19*cm* deep; Figure (1)). Horizontal shortening is achieved displacing a rigid piston at constant velocity perpendicular to the plate margins. A squared grid of passive sand markers enables visualization of the surface deformation.

2.2. 2D Temporal Transition from Subduction to Collision

2D experiments were conducted to investigate the role of preceding subduction in the beginning of collision, and in particular to determine the physical parameters that drive collision processes. The experiments are characterized by the subduction of an oceanic plate leading to oceanic closure, and then to collision. They are described in details in a previous paper [18]. They illustrate the way continental lithosphere subducts prior to collision, and following oceanic subduction. Indeed, we observed three possible modes of slab deformation, i.e., ranked by deformation magnitude, (i) low deformation, (ii) development of viscous instabilities, or (iii) slab break-off. We observed that the greater the deformation magnitude, the shorter is the delay between oceanic closure and continental collision. In other words, the possibility for the continent to subduct is related to the pull exerted by the previously subducted oceanic lithosphere and, therefore, to the way the slab deforms at depth.

Within the Arabia-Eurasia collision zone in Iran, the geodynamics is characterized by 2*D* deformation process in the Northwestern and central Zagros, e.g. [11], but require considerations about the third dimension at the sides of the system, e.g., at the transition between Zagros and Makran, e.g. [19], see Figure (2).

2.3. 3D Spatial Transition from Subduction to Collision

Consequently it is important to determine what controls at depth the superficial features at a spatial transition between subduction and collision. We investigated these 3*D* effects in analogue experiments, cf. [18, 21].

In the reference experiment, see Figure (3), a narrow 3*cm-large* ocean (equivalent to roughly 200*km* in nature) initially separates the indenter from the main continent. Under this condition the subducting plate does not deform much at depth. During the 12 first hours of the experiment, *E-W* folds, i.e., compressional

structures, localize at the weak oceanic plate margin and, subordinately, near the boundaries of the box. This compressional deformation characterizes the initiation of subduction, e.g. [8, 18]. After 12 hours, the oceanic basin closure is completed, causing an increase of the shortening rate to 2*mm/h*, demonstrating the low efficiency of the subducting system during the first phase of subduction in both the eastern and western sides of the experiment. Compressional deformation concentrates on a linear E-trending fold belt that develops in the middle of the plate in correspondence of the end of the model/box boundary sand-less strip, see Figure (3). Only after 29 hours of deformation, the shortening rate in front of the
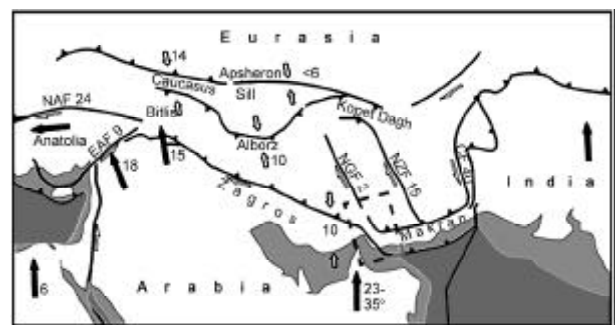

Figure 2. Present-day tectonics of the Middle East, modified after Dercourt et al [7]. White arrows indicate local deformation and solid arrows indicate velocities with respect to stable Eurasia [6, 13, 26]. NAF: North-Anatolian fault; EAF: East-Anatolian fault [13]; NGF: Nayband and Gowk faults [27]; NZF: Neh and Zahedan faults [9, 25, 27]; CF: Chaman fault. [12]. The transition between Zagros and Makran is located inside the gray rectangle.
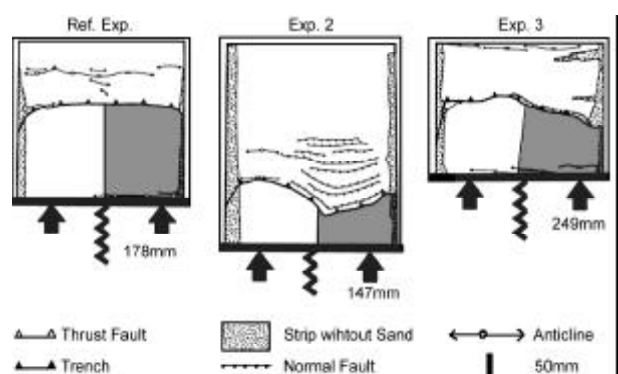

Figure 3. Comparison of experiments. In white are the continents, in gray the ocean. The reference experiment is characterized by low slab deformation. Both the collision part and the subduction part are undergoing compression. Exp. 2 is characterized by break-off under the continental collision, and the transition zone between subduction and collision is very narrow. Exp. 3 is characterized by low slab deformation and high lithospheric strength. In this experiment, the transition subduction-collision is accommodated over the entire experiment.

indenter becomes larger than that accommodated in the area where oceanic subduction takes place. The western domain shortens more, and the difference in shortening rate is accommodated by a N-trending strike-slip zone that links the trench with the main intracontinental zone of deformation, located far from the trench at the centre of the overriding plate. This strike-slip zone accommodates about 20*mm* between 30 and 50*h*, i.e. 1*mm/h* on average [21].

Experiment 2 differs from ref. experiment as the oceanic domain, i.e. the distance separating the indenter and the target continents, is wider (7*cm*). In this manner we obtain a longer oceanic slab that exerts a larger slab pull force. To obtain a maximum level of slab pull, the depth of the box is also increased. Under this condition, the experimental slab must be prone to deform at depth. The initial stage of the experiment is similar to what was observed in the previous experiment, with some *E-W* compressional folds characterizing the subduction initiation occurring in the experiment outside the trench [8, 18]. This phase lasts for around 10 hours producing a shortening of about 10-15*mm*. Afterwards, the subduction zone accommodates efficiently the imposed convergence and the oceanic domain located in front of the indenter is entirely consumed after 18 hours of deformation. During the final stage of oceanic closure, extension appears within the upper plate: E-trending normal faults are observed within the overriding plate. The beginning of continental subduction, as observed in 2*D* experiments [18], does not change significantly the subduction dynamics. Extension lasts up to 26 hours of deformation. The extensional phase of deformation is related to the slab growth at depth. The slab pull resulting from the previous entrance of the dense oceanic plate counterbalances both the effect of the positive buoyancy of the continental part of the slab, and the effect of the piston-imposed shortening [21]. After about 30 hours of model run, under the collisional zone (western part of the experiment), we observe that the slab breaks and that the subducting oceanic lithosphere detaches from the continental part of the slab. Afterwards, the detachment progresses eastward under the boundary between the two continents. Even if it is difficult to establish the rate of lateral propagation of the detachment, it seems to have occurred quite rapidly. As a matter of fact, it was noted that in surface, on the western side of the experiment, E-striking folds and thrust-faults develop just after the slab detachment, reactivating and

inverting normal faults related to the previous stage, see Figure (3). Surface deformation is then strongly influenced by the detachment process. After this break-off, the shortening in front of the indenter reaches a rate of 2.8*mm/h*, accommodating 65% of the total amount of convergence. On the eastern side, conversely, the speed of the oceanic subduction increases with a maximum velocity of about 10*mm/h*, twice the convergence velocity. It results in a rapid back-arc extension, see Figure (3). It was observed that till the end of the experiment, the break-off of the slab remains confined to the continental collision zone, in front of the indenter. This deep behavior increases dramatically the pull exerted by the rest of the oceanic slab on the active oceanic subduction, explaining the large amount of back-arc extension in the western part of the experiment. The contrast between shortening in front of the indenter, and extension above the oceanic subduction zone, is responsible for the appearance of the indenter-like geometry of the plate boundary, cf. [21].

Experiment 3 differs from experiment 2 by larger plate strength only. In this manner we obtain a long oceanic slab, as that of Exp. 2, that exerts a large slab pull force, but the possibility of break-off was avoided. Again, at first the plates undergo compressional stress that is the cause for the development of folds at both North and South boundary of experiment (0-16*h*). The second phase of simple subduction is not marked by superficial deformation. Oceanic closure is completed at around 30*h*, followed by continental subduction in the west whereas to the east subduction pursues normally. Tiny compression occurs in the western part of the box before 44*h*. It is followed by moderate shortening and little compressional deformation, marked by folding at box boundaries and near the trench. During the same time strong, but localized, extension occurs to the east, causing the development of 2 large grabens within the northern continent, see Figure (3). As a consequence of the competition between subduction and collision process the entire northern plate (8*cm-large* at 56*h*) is rotating. At 56*h* of experiment the total rotation is estimated to be between 2° and 12° clockwise from West to East. This rotation results from the competition between subduction and collision processes. It is noteworthy that it involves the entire upper plate without any discontinuity between east and west as observed in the previous experiments.

In summary, our results show that the way the upper plate deforms during indentation depends much

on the characteristics of the subduction system and on the history of subduction. Comparison between the reference experiments highlights the dependence of the pattern of collision and deformation in $3D$ on the way the subduction process develops. The reference experiment demonstrates that the plate boundary is likely to absorb several hundreds of kilometers of continent-continent convergence before an indenter-like geometry appears. In the $3D$ configuration, the subduction of the indenting continent is favored both by the pull of the previously subducted oceanic plate, and by the pull resulting from the lateral active oceanic subduction. Only during the last phases of this experiment, the different efficiency of the subduction system is accommodated in the surface with internal deformation and/or by the rigid rotation of the upper continental block.

If we allow for a larger subduction system (larger initial ocean width, Experiments 2 and 3), the slab pull level on the subducting slab can increase up to the point that the slab breaks [18]: It occurs in Exp. 2 but not in Exp. 3. The lateral propagation of this process (several *cm/yr*) results in a tremendous concentration of the slab pull effect at the tip of the propagating tear [30]. This, in turn, may induce a large-scale back-arc extension above the oceanic subducting plate [4, 28]. This process favors the appearance, in Exp. 2, of an indentation-like geometry between the two lithospheric plates, whereas in Exp. 3, the lack of slab detachment does not allow the development of such geometry. Then, in both Exp. 2 and Exp. 3, the entrance of the indenter within the large continent results on the one hand from the shortening accommodated in front of the indenter, but also from the southern motion of the large continent on the sides of the indenter, and the way the eastern and western part are (de) coupled. In Exp. 2, the slab break-off at moderate depth (ca. 100-200*km* deep) allows decoupling the eastern and western upper plate domains. On the contrary, in Exp. 3, the slab remains continuous from east to west, and the process related to the transition between subduction and collision are accommodated over the entire upper plate. The transition is progressive from $2D$-collision far west and $2D$-subduction far east.

3. Tectonics of Subduction-Collision Transitions

3.1. Zagros-Makran Transition Tectonics

At Iranian longitude, the Arabian plate is moving northward relative to Eurasia (~20*mm* a-1 according to *GPS* [2, 22 26]). To the east, this relative motion is accommodated by northward subduction under the *E-W* Makran emerged accretionary prism. To the west, it is accommodated partly by the Zagros fold-and-thrust belt and partly by the Alborz/Kopet Dagh deforming zones further north. The transition zone between Zagros and Makran has been the locus of several studies within the French-Iranian collaboration e.g., [1, 2, 15, 19, 29]. We present in the following a synthesis of the major results resulting from the active tectonics study [19, 21] combined with *GPS* measurement and seismotectonics studies.

Satellite images and structural and geomorphic field observations show a distributed deformation pattern covering a wide domain. Five *N* to *NW*-trending major faults were identified. They exhibit evidence for late Quaternary reverse right-lateral slip, and correspond to two distinct fault systems. The Minab-Zendan Fault System (*MZFS*), to the south-west, is trending $N160°E$ and transfers the Zagros deformation to the Makran prism. The *N*-trending Jiroft-Sabzevaran Fault System (*JSFS*), to the north-east, is transferring a part of the Makran convergence to deforming zones more to the North (Alborz/Kopet Dagh), by connecting to other major N-trending strike-slip faults of eastern Iran (e.g. Nayband fault) between Makran in the south and Alborz-Kopet Dagh to the north. Tectonic study and fault slip-vector analyses indicate that the entire zone is currently undergoing a stress field characterized by regionally significant transpressional tectonic regime (oblique reverse strike-slip faulting) with a $N45°E$-trending $s1$, indicating that in spite of its distribution, the deformation is not partitioned within this transpressional zone [19].

The area is characterized by a well-defined succession of quaternary deposit levels. The age of these deposits were estimated by archeological data, regional paleoclimate correlations and constrained by additional in situ $10Be$ dating in a previous study [20]. These deposits exhibit offsets both lateral and vertical, which are evaluated by satellite image analysis, and *GPS* profiles. Thanks to offsets and ages the strike-slip rates associated with each one of the faults are calculated, of the order of 2-3*mm/yr*. Each of the two fault systems has strike-slip rates of about 6*mm/yr*; the strike-slip rate integrated over the whole area being of about 12*mm/yr* [20]. The convergence vector accommodated over the entire area, i.e., the motion of Oman relatively to Jaz-Murian, cf. Figure (4), is about 12*mm/yr* in a direction $N10°E$,
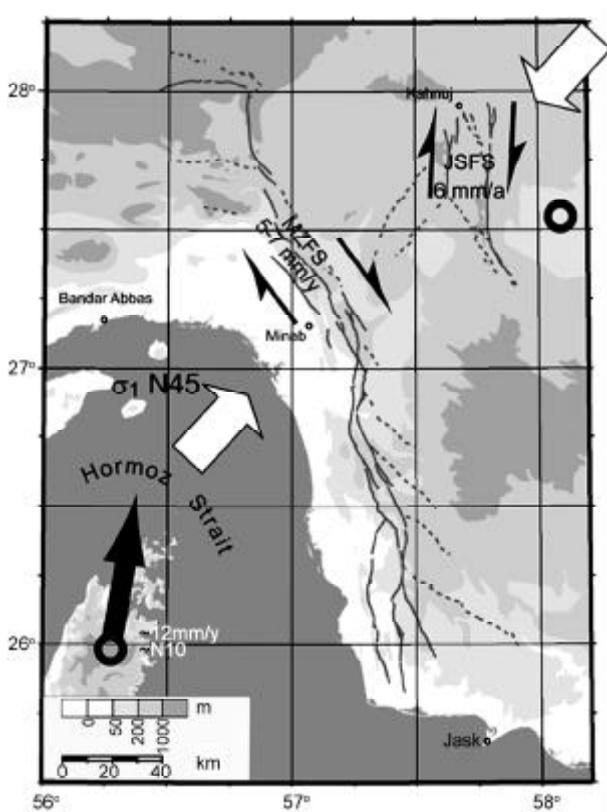
Figure 4. Tectonics of the transition Zagros-Makran. The active fault traces are mapped after Regard et al [19]. The zone is undergoing a homogeneous stress field; the main horizontal compressional axis trends N45°E (white arrows [19]). Two fault systems have been distinguished: the Minab-Zendan fault system (MZFS) and the Jiroft-Sabzevaran fault system (ZJFS). Both are accommodating a strike-slip component of the deforming rate of the order of 6mm/y. Their sum indicates a convergence vector of Munsandam (black arrow) relatively to Jaz-Murian (black open circle) of about 12mm/yr directed ~N10°E [20].

in agreement with *GPS* measurement results obtained by Bayer et al [2] that give evidence for the same motion for about 10*mm/yr* in a direction *N*10°*E*.

Interestingly, *GPS* results indicate a northward motion of Oman of about 25*mm/y* with respect to Eurasia [2, 26], of which we propose that only ca. 10*mm/yr* are accommodated through the Zagros-Makran transition zone. The remaining 10-15*mm/yr* could be taken through another fault system, described by [25], the Neh-Zahedan fault system, lying in the East Iranian Ranges further east, e.g. [19, 20, 26].

Yamini Fard [29] studied the Zagros-Makran transition zone using microseismicity recorded by a temporary seismological network. The recorded seismicity shows a northeast dipping plane, located 10-15*km* under the *MZFS* and 20-30*km* under the *JSFS*. In addition, Byrne et al [5] seismicity study indicates very low dips for the entire Makran subduction plane. In particular, in its western part

(i.e., 250*km* east from the Zagros-Makran transition zone), the subduction plane is only 50*km-deep* under the Jaz-Murian depression which is located 400*km* north of the deformation front. The magmatic arc lies at the north of Jaz-Murian at ca. 500*km* from the deformation front, maybe 70-100*km* above the subduction plane. In conclusion, Yamini Fard [29] shows a north-east dipping plane beneath the Zagros/Makran transition zone that may correspond to the boundary between the Arabian lithosphere and the Iranian one. Thus it should correspond laterally to the subduction plane highlighted by Byrne et al [5].

In abstract, at the transition between Zagros and Makran, deformation is accommodated by two fault systems, within a present-day regional transpressionnal regime with a *N*45°*E*-trending *s*1. On one hand, the Minab-Zendan Fault System (*MZFS*) corresponds to the boundary between the two plates. On the other hand, the Jiroft-Sabzevaran Fault System (*JSFS*) is entirely located in the hanging wall (equivalent to the overriding plate, cf. Figure (5)).
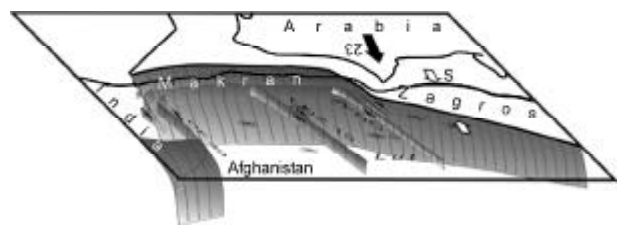

Figure 5. 3D schematic diagram of subduction planes in the Iran-India region. Schematic slabs and lithospheric-scale faults are represented. The slab may be continuous at the transition Zagros-Makran whereas it may be torn away at the transition Makran-Himalayas. Arrows represent convergent vectors, see Figure (2). Asterisks are tertiary volcanoes.

3.2. The Chaman Fault Tectonics

It is interesting to note that the eastern termination of the Makran is also characterized by a subduction-collision transfer zone: The Chaman Fault System (*CFS*). It is constituted by 3 main faults, cf. Figure (5), [12]: The Chaman, Ghazaband and Ornach-Nal faults. The system connects the Makran accretionary prism to the Pamirs (Panjshir fault). Geological studies [3] permit us to determine an about 25-35*mm/yr* strike-slip displacement rate along the Chaman fault system, while global plate kinematics (*NUVEL*-1 model, [6]) allow us to calculate an about 40*mm/yr* rate, for the lateral motion within the whole transition domain. The Chaman fault system is characterized by longer fault segments and an

azimuth closer to the convergence vector than for the Zagros/Makran transition zone.

The two systems differ in age: The Zagros-Makran fault system is young (probably younger than 5*My*), whereas the Chaman fault system is mature, and it is probably developed since at least 20-25*My* [12]. On the contrary to the Zagros-Makran transition zone, the Chaman Fault system efficiently decouples its eastern and western walls.

3.3. Insights from the Models

The two areas considered here (Zagros-Makran transition zone and the Chaman fault zone) bound the same subduction system: The Makran. To the west and to the east the Makran is pretty similar despite little variations, e.g. [5]. It is characterized by a low dip of the subduction of the order of 5 degrees, slightly increasing westward (up to 8°), and by the high elevation reached by the accretionary prism (up to 2000*m*). The strong development and the high elevation of the Makran accretionary prism, although partly explained by the large sediment supply, suggest that the slab-pull force is moderate. This is not in agreement with the old age (at least 80*My*) of the Neo-Tethys oceanic lithosphere, which should imply an important slab-pull force. Nevertheless, this setting cannot explain the differences between Zagros-Makran transition zone and the Chaman fault zone, that are respectively characterised by a wide transition and a sharp transition zone. Interestingly, the Zagros-Makran transition involves a northward motion of the Lut block, see Figure (5), that implies, at the longitude of the western Makran, an accommodation of the convergence partly by the Makran ($19 \pm 2mm/yr$ [26]) subduction and partly by intracontinental deformation zones more to the north ($6 \pm 2mm/yr$ [26]). On the other side, the Helmand block (i,e, Afghanistan), must have once moved northward as attested by the presence of the Hindu Kush range, but is currently fixed to Eurasia, all the convergence being accommodated by the Makran.

The presented experiments provide an interesting overview to highlight the causes of differences between the eastern and western sides of the Makran. Indeed, comparison between experiments 2 and 3 indicates that, instead of a similar initial setting, slab detachment occurrence conducts to major plate reorganization. In particular, no decoupling between east and west is possible without a discontinuity between the eastern and western slab. Following this

conclusion, a continuous slab is expected under the Zagros-Makran transition zone whereas it must be discontinuous between Makran and Himalayas, see Figure (5). Moreover, the flat-lying shallow Benioff suggests that the old and heavy ocean lithosphere is laterally supported by the continental subduction acting like a buoy, in particular at the transition with the Zagros.

As previously mentioned, the main difference between the Makran transitions with the Zagros, in the west, and with the Himalayas, in the east, consists in the age of the two systems of the order of 5 and 20-25*My*, respectively. Thus, it can be considered that the two systems represent two stages within indentation evolution. Indeed, the Himalayas-Makran zone represents a mature transition domain, while the Zagros-Makran transition testifies for a juvenile stage of indentation accommodation. Between these two stages there may have occurred a tearing of the slab in two parts, one under the collision, and the other under the subduction.

In summary, it is proposed that, following a collision the slab can detach or tear away. It results in a tremendous difference in the way both sides accommodate the transition between subduction and collision: By a relative coupling before detachment (Zagros-Makran) or by a decoupling of the subducting and colliding parts after break-off (Makran-Himalayas). This highlights the first-order major role of deep processes on crustal tectonics. Lithospheric plate rheology seems to act only as a second-order role controlling parameter. Actually, in Iran it governs the structures that are reactivated, such as the N-trending Nayband-Gowk fault system that separates central Iran and the Lut Block [19, 27].

4. Conclusions

The indentation of Arabia and India within Eurasia has long been studied in regard to the upper plate tectonics. We propose that deep processes related to Tethyan subduction have been underestimated and they must play a first order role in the way Iran is deforming. Deep processes involved can be a slab break off or, a flexure of the slab without any discontinuity. A discontinuity in the slab (e.g., a detachment) is related to a sharp superficial decoupling zone between the collision and the subduction (ex. Chaman Fault System). Conversely, continuity in the shape of the slab should permit to transfer progressively the deformation from the collision to the subduction domains (ex. Zagros-Makran transition zone).

References

1. Aubourg, C., Smith, B., Bakhtari, H., Guya, N., Eshraghi, A., S., L., Molinaro, M., Braud, X., and Delaunay, S. (2004). "Post-Miocene Shortening Pictured by Magnetic Fabric Across the Zagros-Makran Syntaxis", In Sussman, A.J., and Weil, A.B., eds., Orogenic Curvature: Integrating Paleomagnetic and Structural Analyses: Geological Society of America Special Paper: Boulder, Colorado, 17-40.

2. Bayer, R., Shabanian, E., Regard, V., Yaminifard, F., Vernant, P., Nilforoushan, F., Abbassi, M., Chery, J., Tatar, M., Doerflinger, E., Peyret, M., Daignières, M., Bellier, O., Hatzfeld, D., Mokhtari, M., and Bourlès, D.L. (2002). "Active Deformation in Zagros-Makran Transition Zone Inferred from GPS", Tectonic and Seismological Measurements: EOS Trans. AGU, Fall Meet. Suppl., **83**, Abstract S62B-1188.

3. Beun, N., Border, P., and Carbonnel, J. (1979). "Premières Données Quantitative Relatives au Coulissage du Décrochement de Chaman (Afghanistan du sud-est)", C.R. Acad. Sci. Paris, **288**, 931-934.

4. Buiter, S.H.J., Govers, R., and Wortel, M.J.R. (2002). "Two-Dimensional Simulations of Surface Deformation Caused by Slab Detachment", *Tectonophysics*, **354**, 195-210.

5. Byrne, D.E., Sykes, L.R., and Davis, D.M. (1992). "Great Thrust Earthquakes and Aseismic Slip Along the Plate Boundary of the Makran Subduction Zone", *J. Geophys. Res.*, **97**, 449-478.

6. DeMets, C., Gordon, R.G., Argus, D.F., and Stein, S. (1990). "Current Plate Motions", *Geophys. J. Int.*, **101**, 425-478.

7. Dercourt, J., Zonenshain, L.P., Ricou, L.-E., Kazmin, V.G., Knipper, A.L., Grandjacquet, C., Sbortshikov, I.M., Geyssant, J., Lepvrier, C., Pechersky, D.H., Boulin, J., Sibuet, J.-C., Savostin, L.A., Sorokhtin, O., Westphal, M., Bazhenov, M.L., Lauer, J.P., and Biju-Duval, B. (1986). "Geological Evolution of the Tethys Belt from the Atlantic to the Pamirs Since the Lias, in Aubouin", J., Le Pichon, X., and Monin, A.S., eds., Evolution of the Tethys, **123**, *Tectonophysics* (spec. issue), 241-315.

8. Faccenna, C., Giardini, D., Davy, P., and Argentieri, A. (1999). "Initiation of Subduction at Atlantic-type Margins: Insights from Laboratory Experiments", *J. Geophys. Res.*, **104**, 2, 749-2, 766.

9. Freund, R. (1970). "Rotation of Strike-Slip Faults in Sistan, Southeast Iran", *J. Geol.*, **78**, 188-200.

10. Johnson, M.R.W. (2002). "Shortening Budgets and the Role of Continental Subduction During the India-Asia Collision", *Earth Sci. Rev.*, **59**, 101-123.

11. Keskin, M. (2003). "Magma Generation by Slab Steepening and Breakoff Beneath a Subduction-Accretion Complex: An Alternative Model for Collision-Related Volcanism in Eastern Anatolia, Turkey", *Geophys. Res. Lett.*, **30**, p. 8046, doi:10.1029/2003GL018019.

12. Lawrence, R.D., Khan, S.H., and Nakata, T. (1992). "Chaman Fault, Pakistan-Afghanistan", *Ann. Tectonicae*, Spec. Issue.-Suppl. to VI, 196-223.

13. McClusky, S., Balassanian, S., Barka, A., Demir, C., Ergintav, S., Georgiev, I., Gurkan, O., Hamburger, M., Hurst, K., Kahle, H., Kastens, K., Kekelidze, G., King, R., Kotzev, V., Lenk, O., Mahmoud, S., Mishin, A., Nadariya, M., Ouzounis, A., Paradissis, D., Peter, Y., Prilepin, M., Reilinger, R., Sanli, I., Seeger, H., Tealeb, A., Toksöz, M.N., and Veis, G. (2000). "Global Positioning System Constraints on Plate Kinematics and Dynamics in the Eastern Mediterranean and Caucasus", *J. Geophys. Res.*, **105**, 5695-5719.

14. Mercier, J.-L., Sorel, D., Vergely, P., and Simeakis, K. (1989). "Extensional Tectonic Regimes in the Aegean Basins During the Cenozoic", *Basin Res.*, **2**, 49-71.

15. Molinaro, M., Guezou, J.C., Leturmy, P., Eshraghi, S.A., and Frizon de Lamotte, D. (2004). "The Origin of Changes in Structural Style Across the Bandar Abbas Syntaxis, SE Zagros (Iran)", *Mar. Petrol. Geol.*, **21**, 735-752.

16. Molnar, P. and Tapponnier, P. (1975). "Cenozoic Tectonics of Asia: Effects of a Continental Collision", *Science*, **189**, 419-426.

17. Ranalli, G. and Murphy, D.C. (1987). "Rheological Stratification of the Lithosphere", *Tectonophysics*, **132**, 281-296.

18. Regard, V., Faccenna, C., Martinod, J., Bellier, O., and Thomas, J.-C. (2003). "From Subduction to Collision: Control of Deep Processes on the Evolution of Convergent Plate Boundary", *J. Geophys. Res.*, **108**, 2208, doi:10.1029/2002JB001943.

19. Regard, V., Bellier, O., Thomas, J.-C., Abbassi, M.R., Mercier, J., Shabanian, E., Fegghi, K., and Soleymani, S. (2004). "The Accommodation of Arabia-Eurasia Convergence in the Zagros-Makran Transfer Zone, SE Iran: A Transition between Collision and Subduction through a Young Deforming System", *Tectonics*, **23**, p. TC4007, doi:10.1029/2003TC001599.

20. Regard, V., Bellier, O., Thomas, J.-C., Bourlès, D., Bonnet, S., Abbassi, M.R., Braucher, R., Mercier, J., Shabanian, E., Soleymani, S., and Feghhi, K. (2005a). "Cumulative Right-Lateral Fault Slip Rate Across the Zagros-Makran Transfer Zone: Role of the Minab-Zendan Fault System in Accommodating Arabia-Eurasia Convergence in SE Iran", *Geophys. J. Int*., **162**, 177-203.

21. Regard, V., C. Faccenna, J. Martinod, and Bellier, O. (2005b). "Slab Pull and Indentation Tectonics: Insights from 3D Laboratory Experiments", *Phys. Earth. Planet. Int.*, **149**, 99-113.

22. Sella, G.F., Dixon, T.H., and Mao, A. (2002). "REVEL: A Model for Recent Plate Velocities from Space Geodesy", *J. Geophys. Res.*, **107**, p. doi:10.1029/2000JB000033.

23. Sébrier, M. and Soler, P. (1991). "Tectonics and Magmatism in the Peruvian Andes from Late Oligocene Time to Present", in Harmon, R.S., and Rapela, C.W., eds., Andean Magmatism and Its Tectonic Setting, **265**: *Geol. Soc. Am. Spec. Pap.*, Boulder, 259-278.

24. Shen, F., Royden, L.H., and Burchfiel, B.C. (2001). "Large-Scale Crustal Deformation of the Tibetan Plateau", *J. Geophys. Res.*, **106**, 6793-6816.

25. Tirrul, R., Bell, I.R., Griffith, R.J., and Camp, V.E. (1983). "The Sistan Suture Zone of Eastern Iran", *Geol. Soc. Am. Bull.*, **94**, 134-150.

26. Vernant, P., Nilforoushan, F., Hatzfeld, D., Abbassi, M., Vigny, C., Masson, F., Nankali, H., Martinod, J., Ashtiani, M., Bayer, R., Tavakoli, F., and Chéry, J. (2004). "Contemporary Crustal Deformation and Plate Kinematics in Middle East Constrained by GPS Measurements in Iran and Northern Oman", *Geophys. J. Int.*, **157**, 381-398.

27. Walker, R. and Jackson, J. (2002). "Offset and Evolution of the Gowk Fault, SE Iran; A Major Intra-continental Strike-Slip System", *J. Struct. Geol.*, **24**, 1677-1698.

28. Wortel, M.J.R. and Spakman, W. (1992). "Structure and Dynamics of Subducted Lithosphere in the Mediterranean Region", *Proc. Kon. Ned. Akad. v. Wetensch.*, **95**, 325-347.

29. Yamini Fard, F. (2003). "Sismotectonique et Structure Lithosphérique de Deux Zones de Transition Dans le Zagros (Iran) : la Zone de Minab et la zone de Qatar-Kazerun", Université J. Fourier - Grenoble I, France.

30. Yoshioka, S. and Wortel, M.J.R. (1995). "Three-Dimensional Numerical Modelling of Detachment of Subducted Lithosphere", *J. Geophys. Res.*, **100**, 20223-20244.